"SCIENCE & TECHNOLOGY OF WATER RESOURCES»

NATIONAL TECHNICAL UNIVERSITY OF ATHENS

INTERDISCIPLINARY
INTERDEPARTMENTAL
POSTGRADUATE STUDIES
"SCIENCE & TECHNOLOGY
OF WATER RESOURCES "

Stochastic analysis and simulation of multiple time scale of wind speed in Greece (Extended abstract)

Dimakos A. Ioannis

Athens, March 2014

Supervisor: Professor D. Koutsoyiannis

Extended abstract

Introduction

Wind is a fundamental atmospheric variable, which affects weather forecasting, aircraft and marine transportations - operations, construction projects, growth and metabolism rate of many plant species and countless other implications. It is commonly measured with anemometers (m/s), but also can be classified using the older Beaufort scale, which is based on people's observations of specifically defined wind affects. It is governed by chaotic behavior and is therefore difficult to predict. This fact implies that any infinitesimal changes to the initial conditions, will cause completely different behavior to the phenomenon. However, wind behavior, can predicted with some degree of credibility or with a confidence interval. Of great importance is the predictability of wind speed, for areas that extremes occurred, such as hurricanes and typhoons.

Numerous factors and situations affect wind speed on varying time scales, such as pressure gradient, Rossby waves, jet streams and local weather conditions. This fact implies the chaotic behavior of the wind, as it is affected by other meteorological variables, at spatial and temporal variability. Moreover, notably links have been found between wind speed and wind direction, corresponding to the pressure gradient of the atmosphere.

Pressure gradient is a term to describe the difference in air pressure between two points in the atmosphere or on the Earth's surface. It is vital to wind speed, because the greater the difference in pressure, the faster the wind flows to balance out the variation. The pressure gradient, when combined with the Coriolis Effect and friction, also influences wind direction.

Rossby waves are strong winds in the upper troposphere. These operate on a global scale and move from West to East, known as Westerlies. The Rossby waves are themselves a different wind speed from what the experience reveals as in the lower troposphere.

Local weather conditions play a key role in influencing wind speed, as the formation of hurricanes, monsoons and cyclones, as freak weather conditions, can drastically affect the velocity of the wind. (C.Michael Hogan, 2010. *Abiotic factor. Encyclopedia of Earth. eds Emily Monosson and C. Cleveland. National Council for Science and the Environment*. Washington DC)

Statistical – stochastic data analysis

In this thesis, it is realized the statistical - stochastic treatment of the wind speed, on monthly and daily time scale. Data analyses were extracted from site: http://www.ncdc.noaa.gov/cdo-web/, which is a global database of climatologically variables. Wind speed data at Greece, with subsequent data sets, direction and gust, were extracted. The selected analysis stations (Fig. 1, 3), were all the available from the site (83), five of which had no data, thus remain 78. Then the processing of six of the remaining stations had many shortcomings and limited data, thus may not be suitable for processing and reliable conclusions (Fig. 2, 4). For statistical - stochastic process of wind speed, it was initially necessary, processing data in an appropriate format, in order to extract time series.

Data consisted on time series of irregular time step, with shortages of measurements and so it was necessary to formulate time series for further treatment. Statistical features which were

calculated to reveal the behavior of wind speed at Greece were the basic statistical characteristics of a variable, as well as, the calculation of specific estimators and it became obvious the variability of wind speed, at different time scales. Furthermore, it became obvious, the intermittent behavior of wind speed, at all time scales. The shorter the time scale was examined, the less intermittent behavior of the variable revealed. Finally, at monthly time scale, it became clear the cyclostationary behavior of the wind.

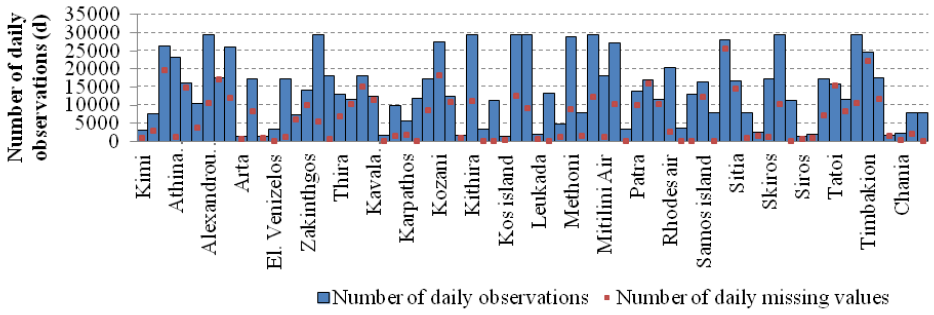

Figure 1: Data stations at Greece, which were analyzed, at daily time scale.

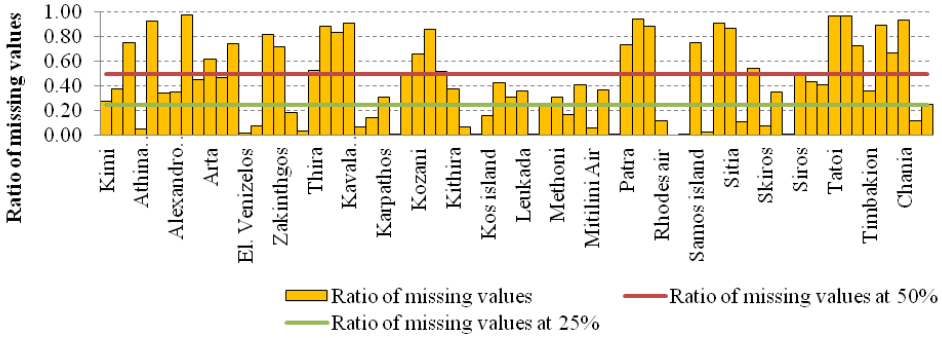

Figure 2: Ratio of missing values at daily time scale.

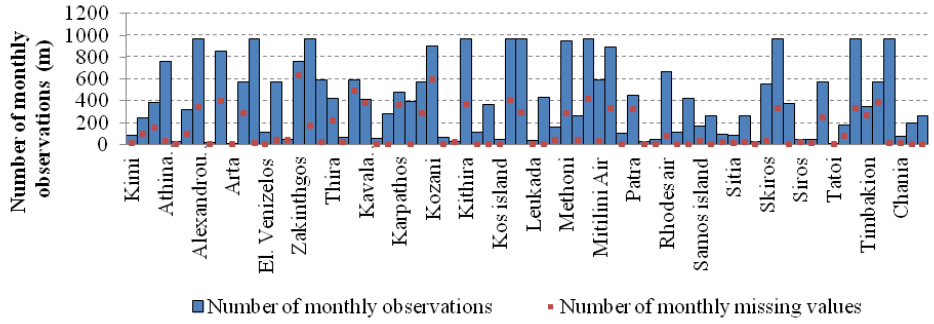

Figure 3: Data stations at Greece, which were analyzed at monthly time scale.

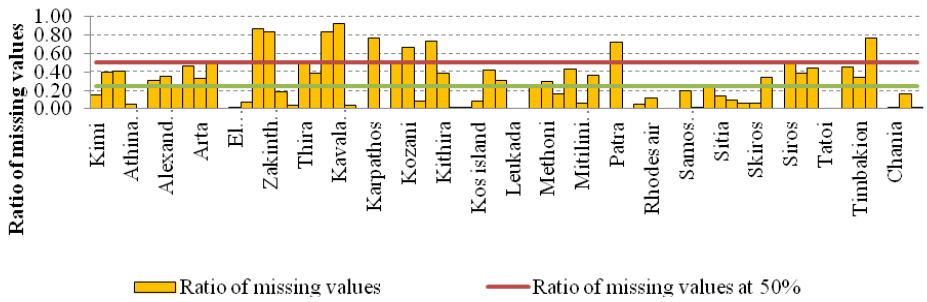

Figure 4: Ratio of missing values at monthly time scale.

Wind speed

Wind speed time series were elaborated, in order to determine monthly averages from each station and also reckon their spatial and temporal variance at the area of interest. To this end, wind speed (m/s) monthly maps were designed (Fig. 5), in order to reveal the monthly wind speed behavior, at Greece.

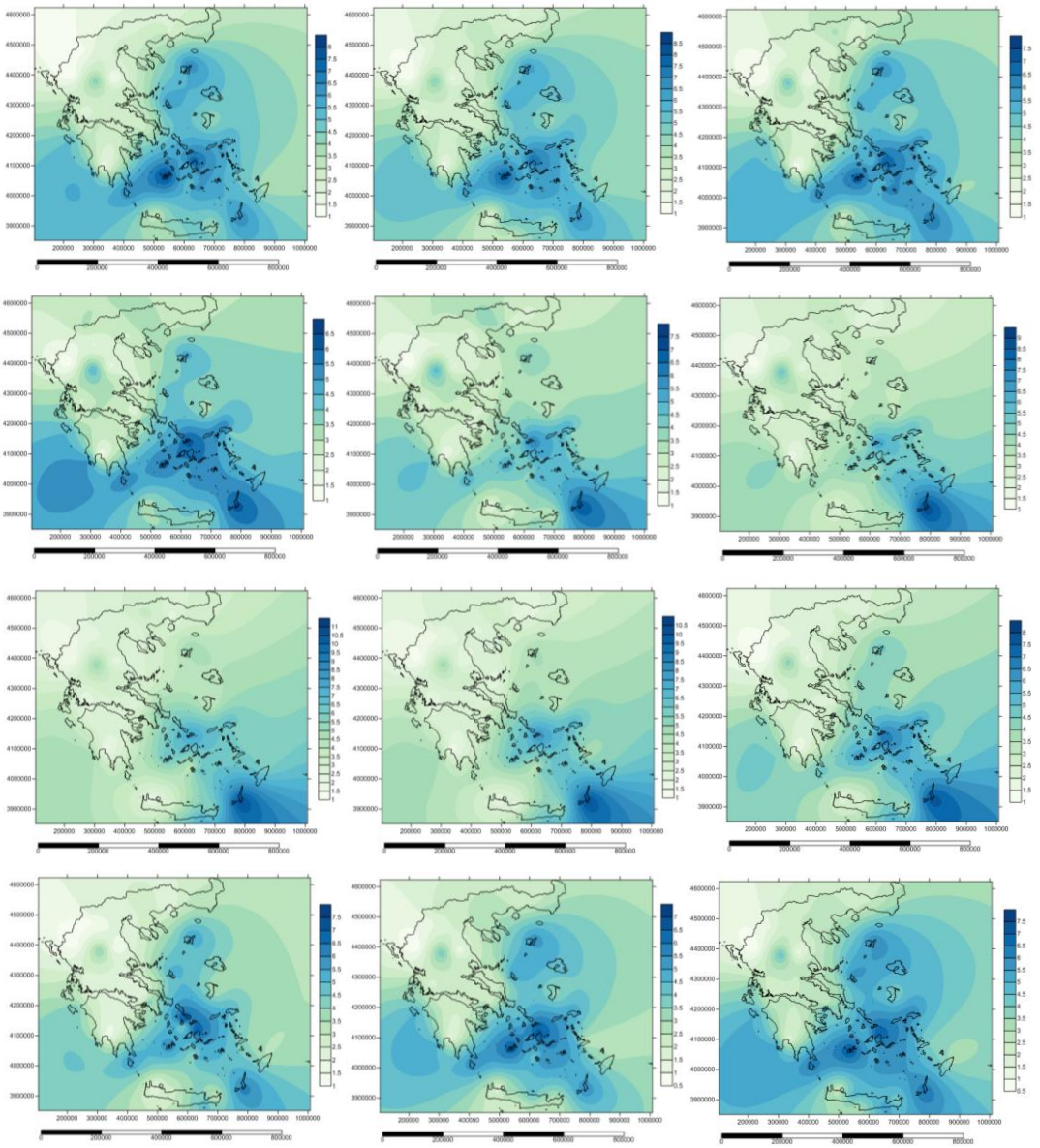

Figure 5: Spatial and temporal disperse of monthly average wind speed from January (top left) to December (bottom right, following right direction when reading).

Wind direction

Wind direction was calculated for all the 36 stations with the available data, by estimating the monthly average wind direction from each station. Direction data, depicted from where wind blows at degrees (^{o}), so that for instance, wind directions of 360^o were concerned northern ones. But, as direction is fragment to the space of [0^o, 360^o] and furthermore, as direction is a vector variable, average should be carefully estimated. The average of two directions that blows from e.g. 360^o and 5^o, will be about 180^o, the opposite direction from the real one. So that, special gauges took place, keeping in mind the above mentioned task and furthermore as

direction data were given from where the wind blows, in order to reveal the truly direction of wind, additions and deductions should be done from ±180^{o} if variable is grater or smaller than 180^{o}. The results revealed (Fig. 6) that most of the percentage of wind's directions in Greece (about 44%) is northern ones and the season that this behavior occurred is winter and specifically corresponded at February (58%).

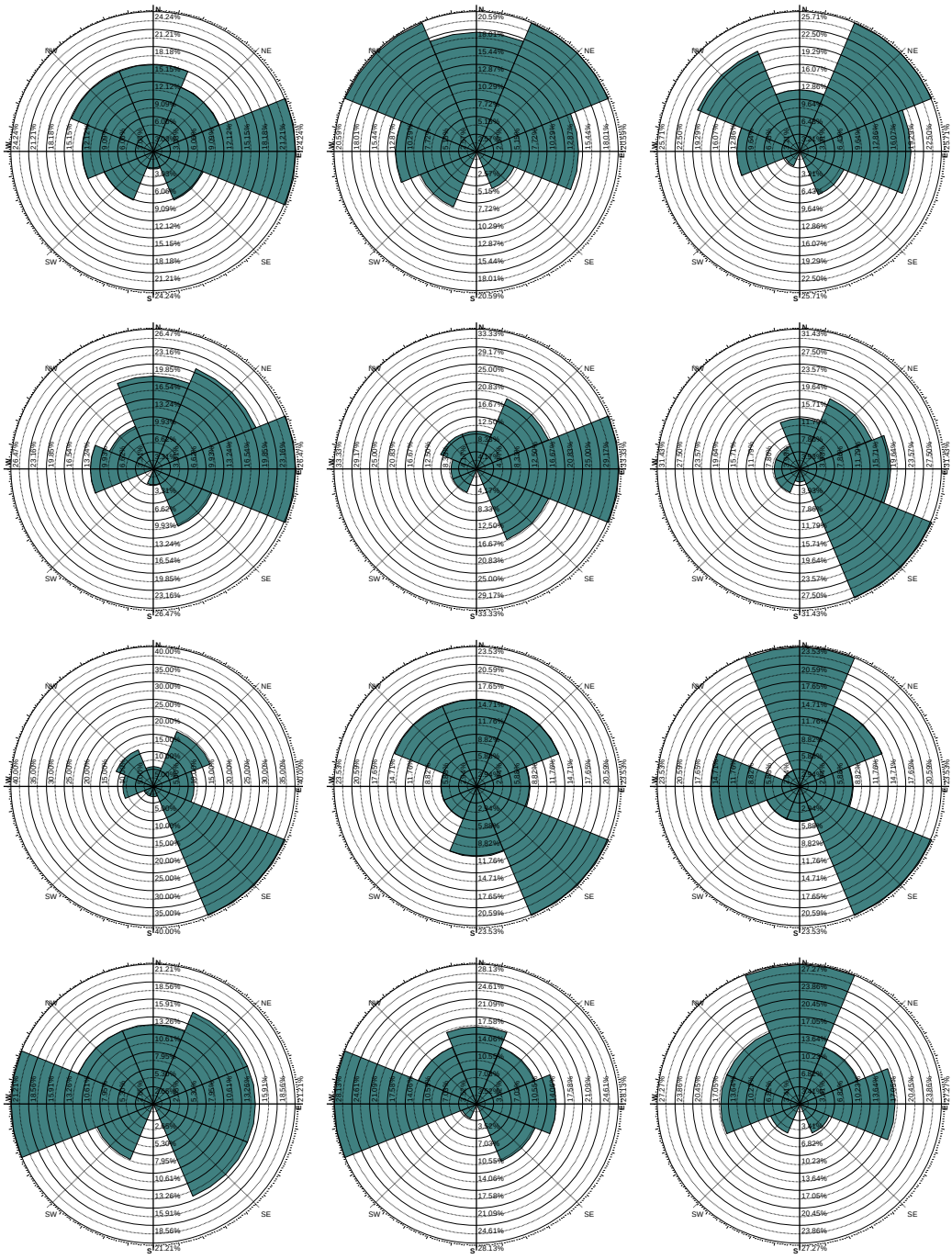

Figure 6: Direction of wind speed at degrees (^{o}), from 36 stations of Greece.

Distribution fitting

Statistical characteristics of wind speed examined at the area of interest, were: mean, standard deviation (variance), coefficient of autocorrelation and autocovariance of time series, at daily and monthly time scale. Furthermore climacograms and power spectras were extracted, for each station, at the same time scale, as the above mentioned. All the important features, that

were necessary for the stochastic processes of wind speed, were derived, by considering all the above statistical treatment, which led to draw conclusions, about the general behavior of this variable.

Hydrognomon software was used for the statistical analysis of the variables, under which the distribution that best fits to the empirical wind speed data (Fig. 7) was assumed to be Weibull, as well as Gamma distribution, which fitted very well to the historical sample, with prevalence of Weibull distribution (Fig. 8) to describe wind speed at both daily and monthly time scale.

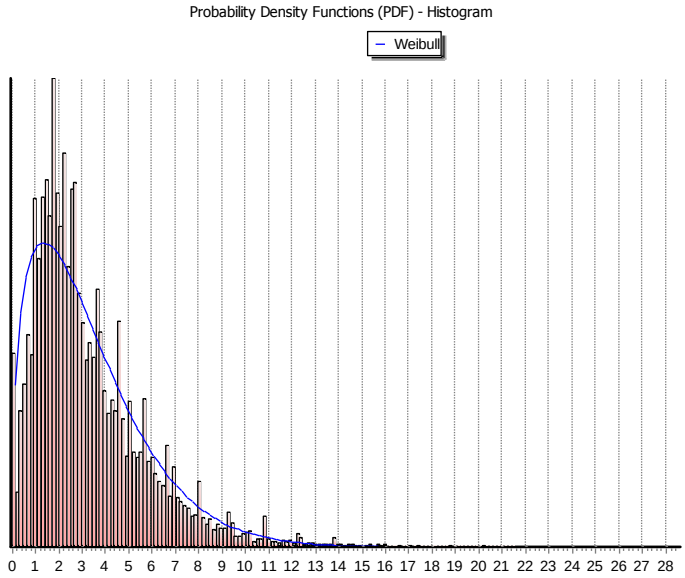

Figure 7: Histogram of the empirical data from Alexandroupoli station, fitted with the Weibull distribution (Hydrognomon).

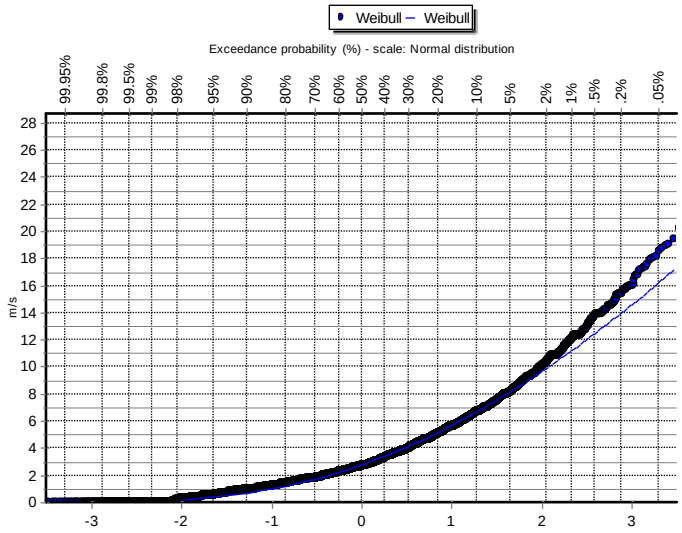

Figure 8: Empirical data and fitting of the Weibull distribution, for Alexandroupoli station (Hydrognomon).

Wind Gust

Empirical data of wind gust were treated (Fig. 9) and specific distributions were fitted to the observed ones and it was concluded that, the distributions which best fits to the wind gust, were GEV max and Gumbel max, with prevalence of GEV max (Fig. 10). Also, from these calculations, were considered the maximum of the maximum values (maxima of maxima) in groups of 200, 100, 50 and 10 values respectively (right tail of distribution) and in all of the above cases it was concluded that these extreme values were adjusted to the exponential distribution. The above conclusion was resulted from the initial configuration of the sample in ascending order, as displayed the values on a diagram and fitting a trend line to the data. The suitability of the adjustment was tested by the RMSE criterion and in all cases it was showed that the value was approximately 0.85 which appeared very good adaptation to the voltage of the sample.

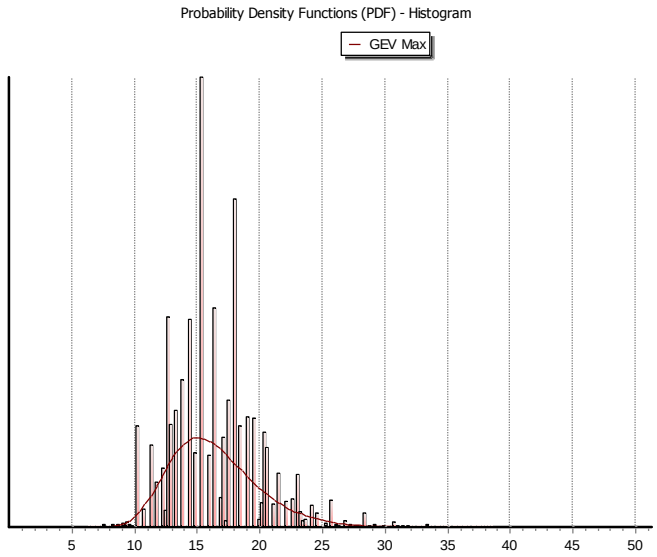

Figure 9: Histogram of the empirical data from Alexandroupoli station, fitted to GEV max distribution (Hydrognomon).

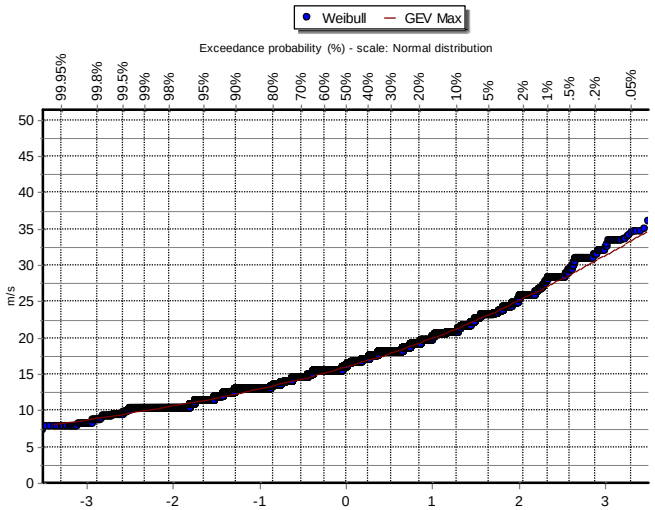

Figure 10: Empirical data and fitting to GEV max distribution, from Alexandroupoli station (Hydrognomon).

As far as, gust data concerned, for a specific number of stations and for a specific observed period, it was held the treatment of the variable, for further comparison with wind speed, at daily time scale, in order to find a relationship between these two variables. Estimations were held at daily time scale and at the same day, so the conjunctions between winds speed and gust, to be directly estimated. Mean (Fig. 11) and standard deviation (Fig. 12), of the differences and the ratio, were calculated, between the two variables, in order to reveal, if they were characterized by a common statistical - stochastic pattern (Fig. 13).

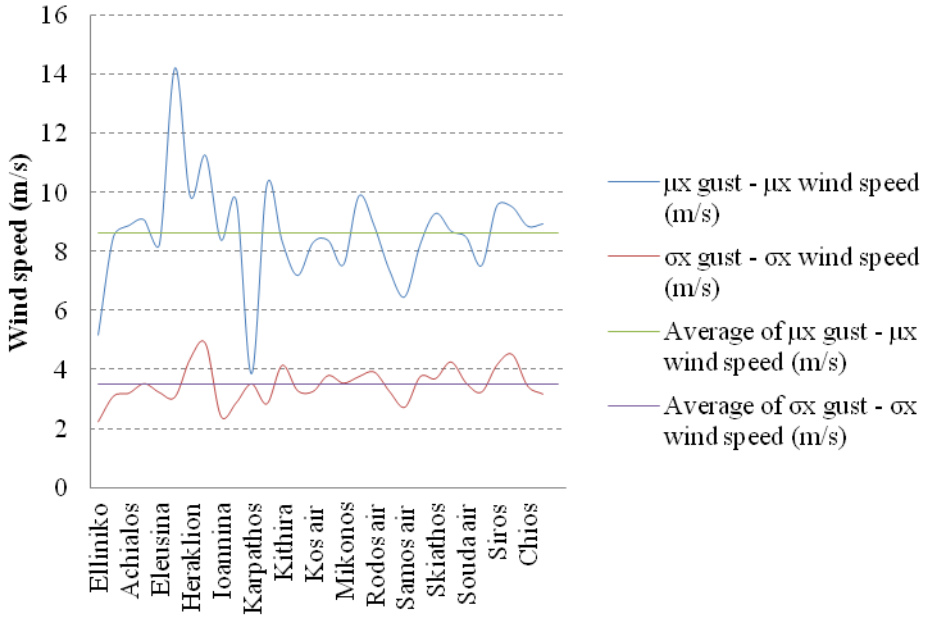

Fig. 11: Mean (μ_x) and standard deviation (σ_x) of the differences, between gust and wind speed at the same day, at m/s.

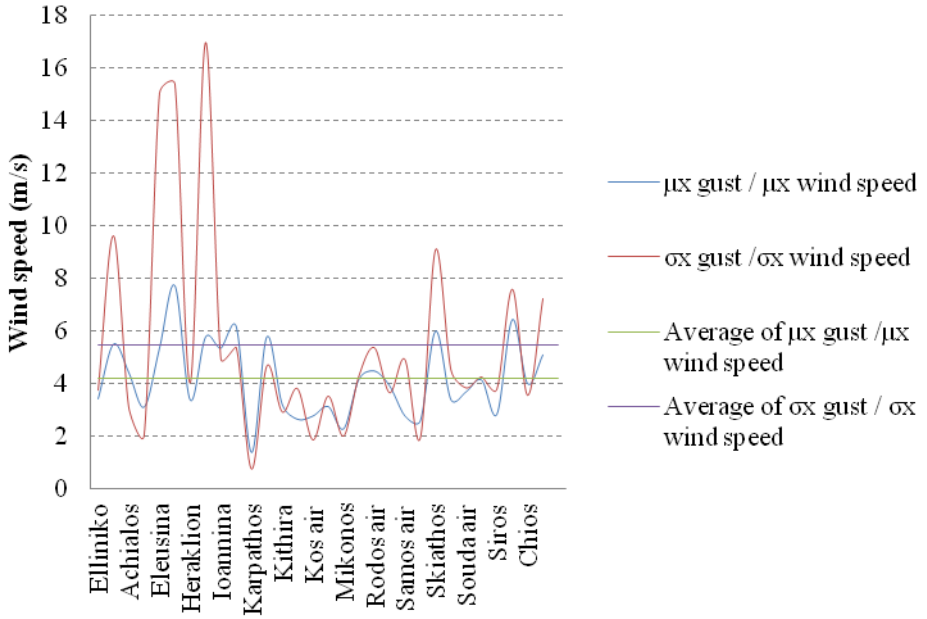

Fig. 12: Mean (μ_x) and standard deviation (σ_x) of the ratio, between gust and wind speed at the same day.

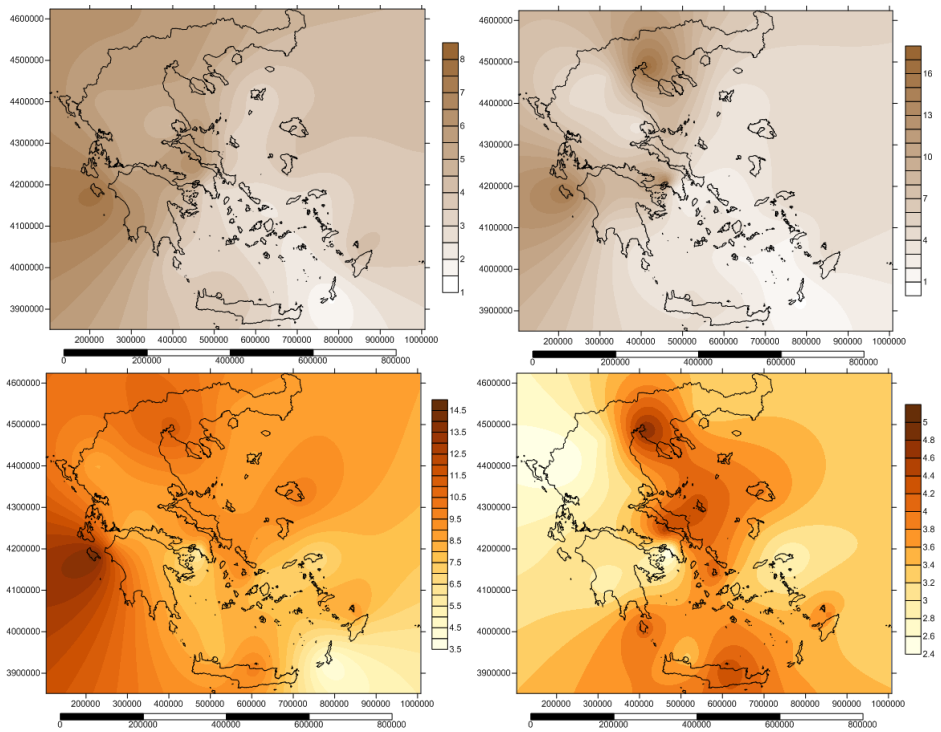

Figure 13: Mean and standard deviation of ratio (upper raw) and differences (lower raw), between gust and wind speed, at the same day.

Reanalysis data

Furthermore, treatment of reanalysis data were occurred, for specific stations, due to the measurement period and results were compared with the ones of 30 stations of observed data, to deduce about the reliability on actual measurements (reanalysis). For this purpose, it was performed the calculation of cross correlation of the stations, between the observed and reanalysis data, so the comparison of cross correlation of the stations was occurred, separately, for each station and between stations (Fig. 14), for each data cross correlation, block. This calculation was occurred to quantify the reliability of reanalysis data and finding the use of such data to draw firm conclusions. Cross correlation analysis between observations and reanalysis data revealed good correspondence (values until 0.85) especially to the areas that extreme had occurred and the main result, from the above mentioned analysis, was the fact that values of reanalysis data were spatially dispersed such as observations. Reanalysis data showed the same areas of extreme wind speed as observations, so they are very helpful in cases of observation's lack, when studying a specific area.

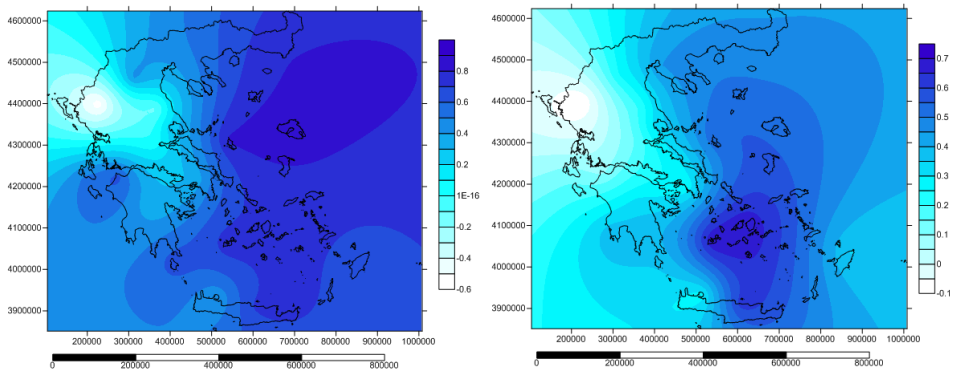

Figure 14: Cross correlations between observed data and reanalysis one (on the left) and cross correlations of the cross correlations between observed data and reanalysis one (on the right).

Catastrophic events at Greece due to extreme winds

Specific maps were exported, for the most catastrophic events at Greece for every month (Fig 15), related to the extreme wind speed events, in order to show the spatial and temporal dispersion of these phenomena at Greece and find areas where such phenomena occur frequently. Of major importance, for the above process, was the period of time that these phenomena occurred, which results to some conclusions about wind speed trend analysis. Monthly time scale maps were developed, which emphasize to the spatial and temporal distribution of the most catastrophic events, due to the extreme wind speed.

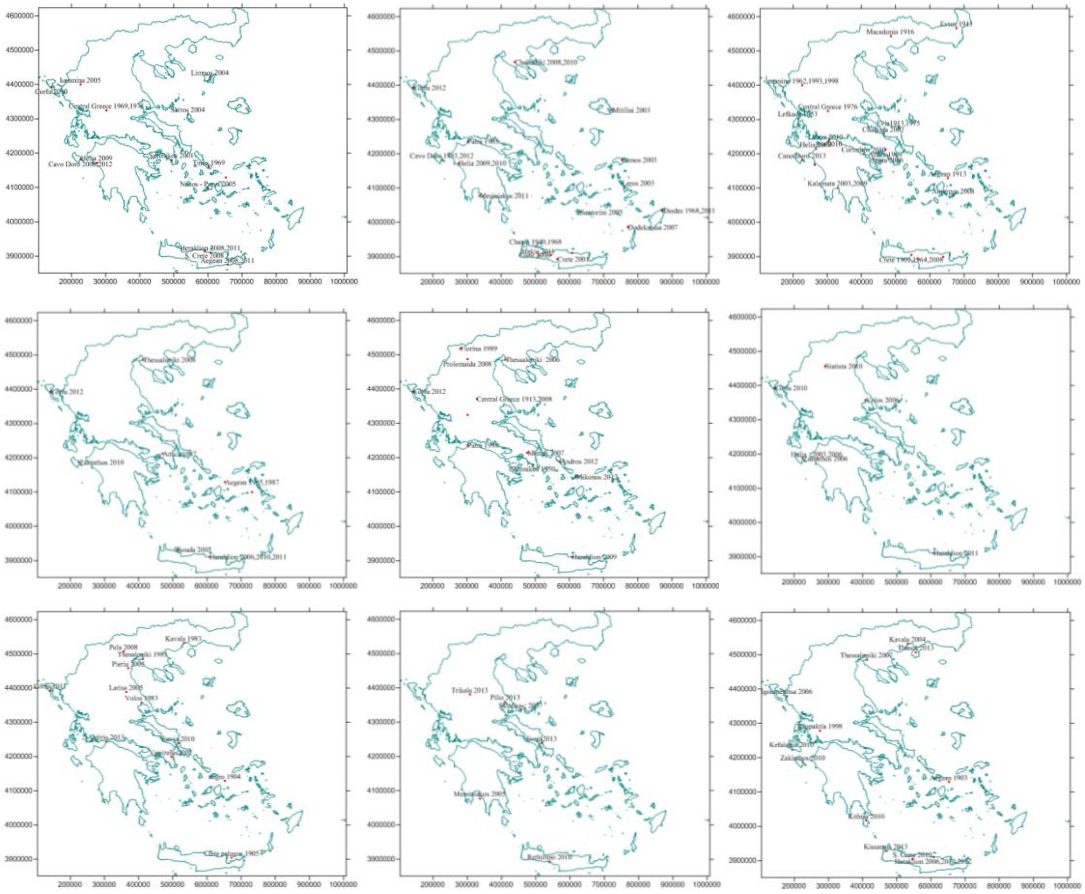

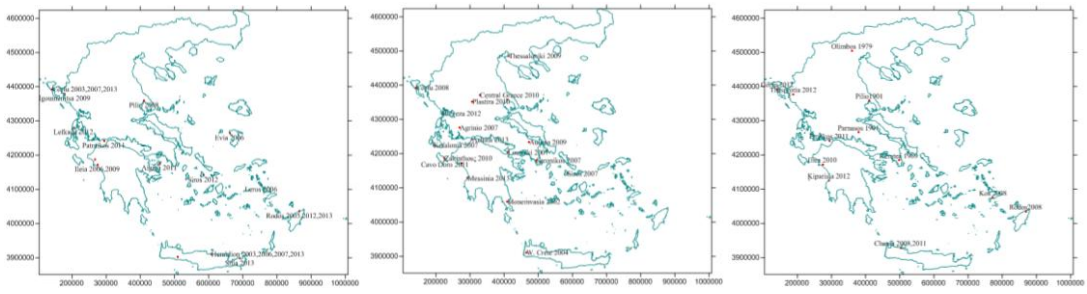

Figure 15: The most catastrophic events, due to extreme wind speed per month, at Greece, from January (top left) to December (bottom right, following right direction when reading).

Wind speed trends at period (1970-2013)

Specific stations were used, at common measurement period, for wind trend analysis, in order to find the past conduct of wind for the observed period and to draw conclusions about wind speed trends for that period at specific areas. Trend analysis was extracted by linear regression to the empirical data, for every month. For a better realization of results, maps were designed, in order to depict the positive and negative trends for specific areas, all over Greece terrain (Fig 16).

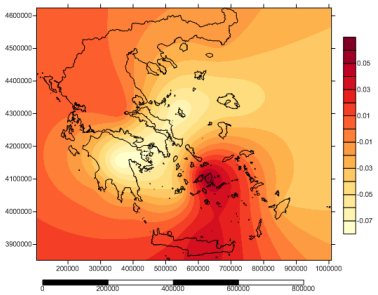

Figure 16: Trends of wind speed at Greece, at the period (1970-2013). Positive trends (red) and negative trends (yellow).

Furthermore, the examined period was split into two smaller ones, in order to extract, differences, at divided examine periods. So the period (1970-2013) was separated into the periods (1970-1990) and (1991-2013) and maps were designed (Fig. 17), in order to reveal any differences with the first examined period. The trends of the examined variable then showed a different view at the period (1970-1990) and almost the same disperse at the period (1992-2013).

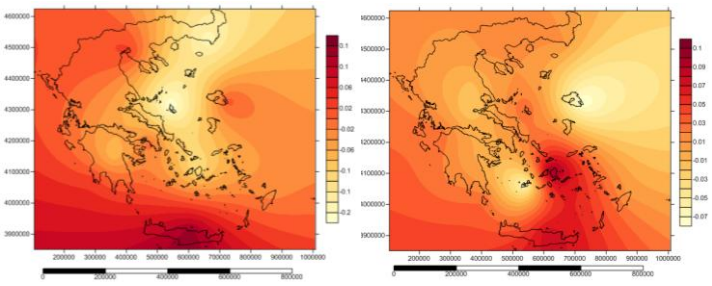

Figure 17: Trend analysis of wind speed variable, at m/s/month, at the periods (1970-1990) (on the right) and (1992-2013) (on the left).

Theoretical wind energy potential at Greece

Theoretical wind energy potential per month (Fig. 18) was carried out, in plants of (W/m^2), from monthly and daily aggregated data sets, and it was performed comparison between them, showed whether they assume same or different results. For a more comprehensive analysis, of the areas due to the quantification of the (theoretical) potential energy and reliability in areas with large (theoretical) potential energy, calculations were carried out, in order to find the percentages of maximum winds, at each region (percentages 1-5-10-20 -30%) at both daily and monthly time scale and vice versa (the percentages of prevailing winds, with specific speed limits at daily and monthly time scale), in order to present a more obvious conclude, about the areas that really have large percentages of high wind speed.

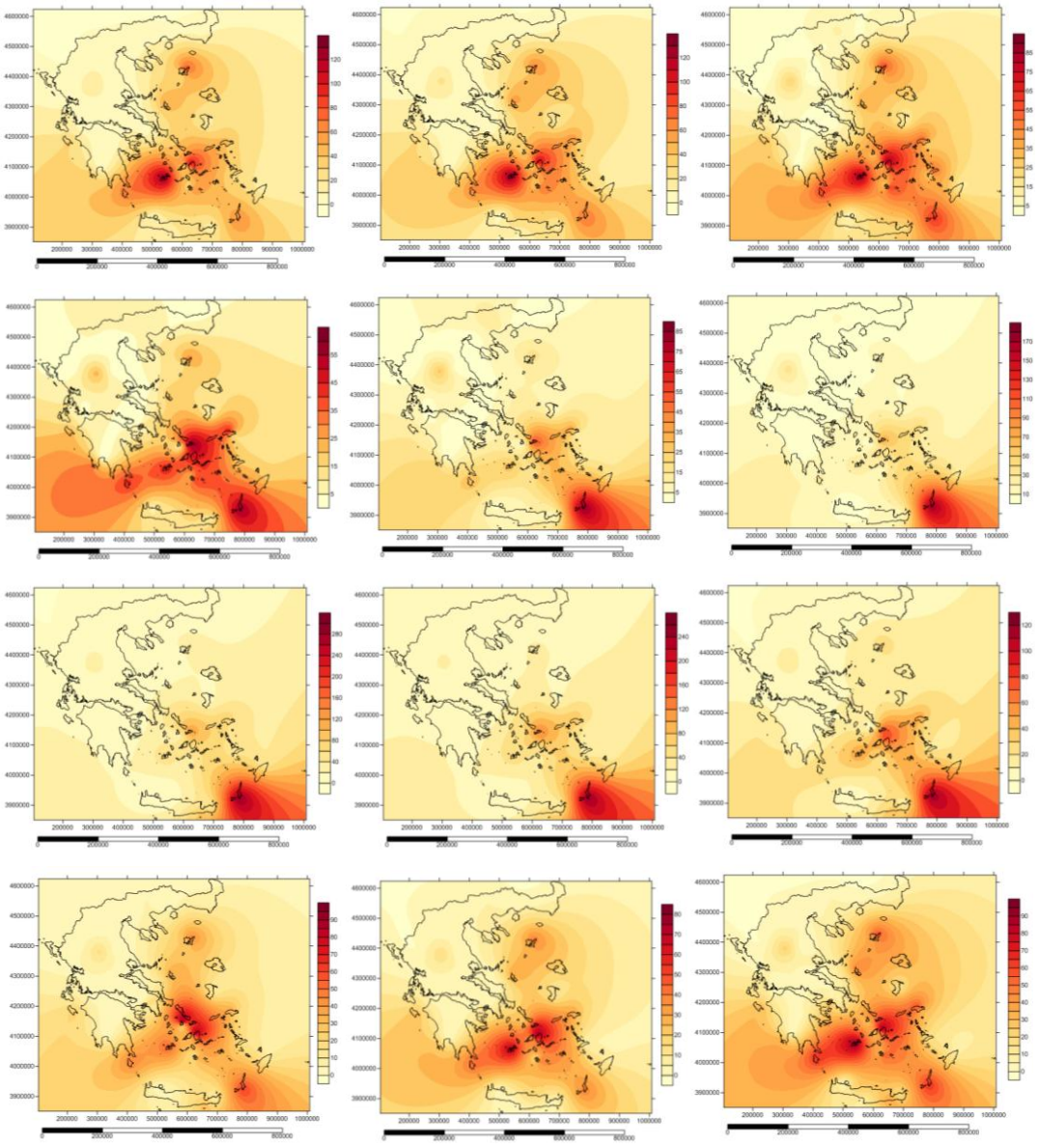

Figure 18: Theoretical wind energy potential for every month (W/m^2), from monthly aggregated time series, from January (top left) to December (bottom right, following right direction when reading).

Weibull shape (k) and scale (c) parameters.

Adjusting the Weibull distribution to the observed data, it were estimated the shape (Fig. 19) and scale (Fig. 20) parameters of the distribution (k, c) at monthly and daily time scale and also it was revealed their dispersion in the entire country, as well as examined, if these

parameters, follow any spatial or seasonal form. Also, from the observed data of wind direction, it was calculated the spatial and temporal behavior of this variable at Greece, to draw conclusions about the rate of the steering winds at a monthly time scale, as well as, for seasonal and annual one.

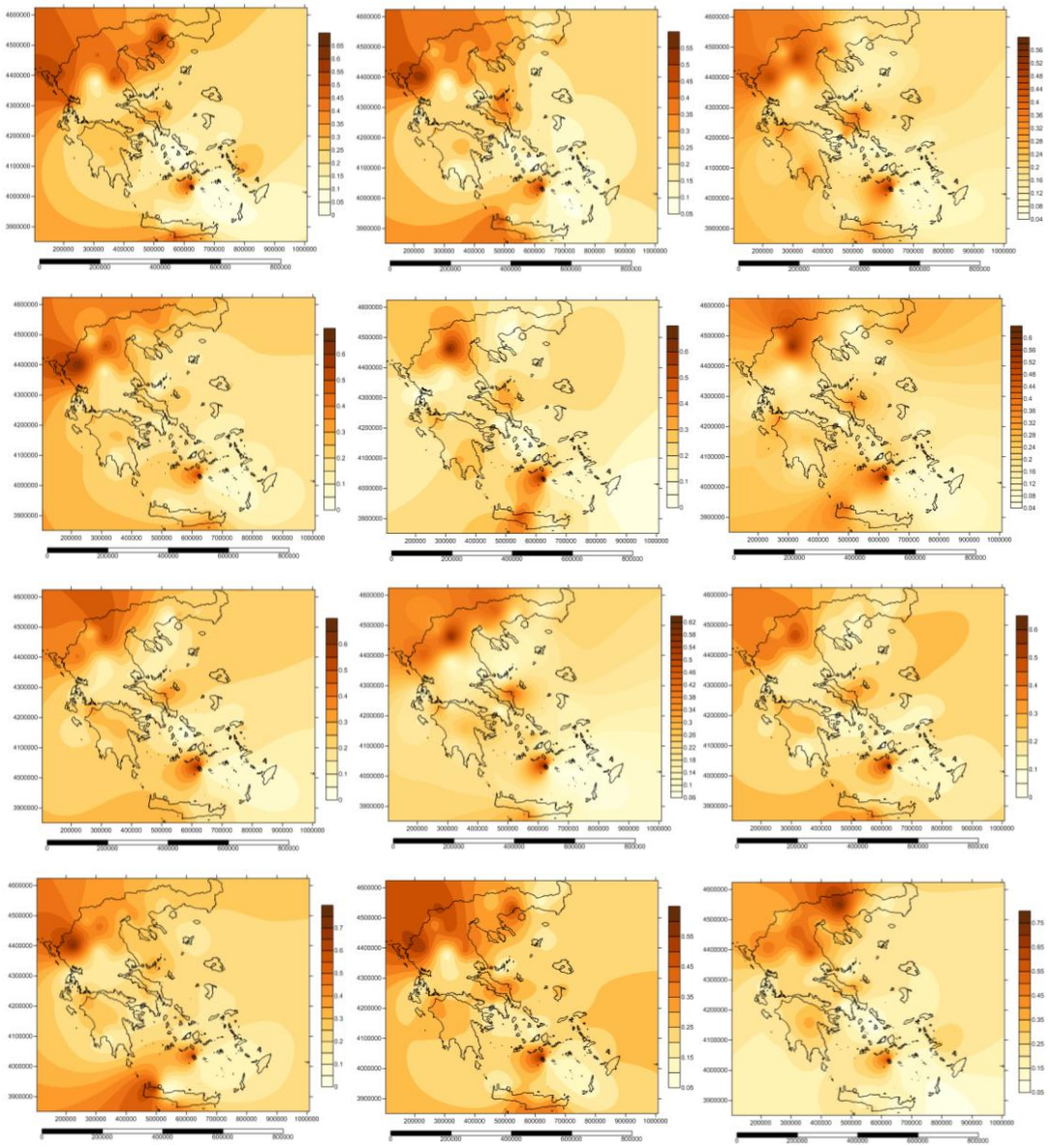

Figure 19: Disperse of the Weibull shape parameter (k), from monthly aggregated time series, at Greece, from January (top left) to December (bottom right, following right direction when reading).

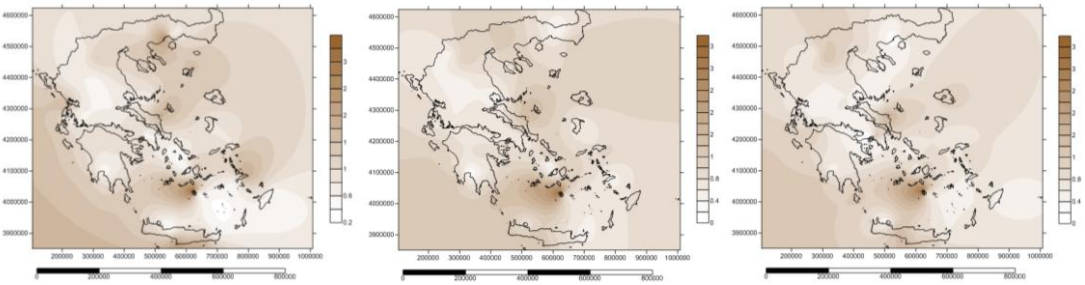

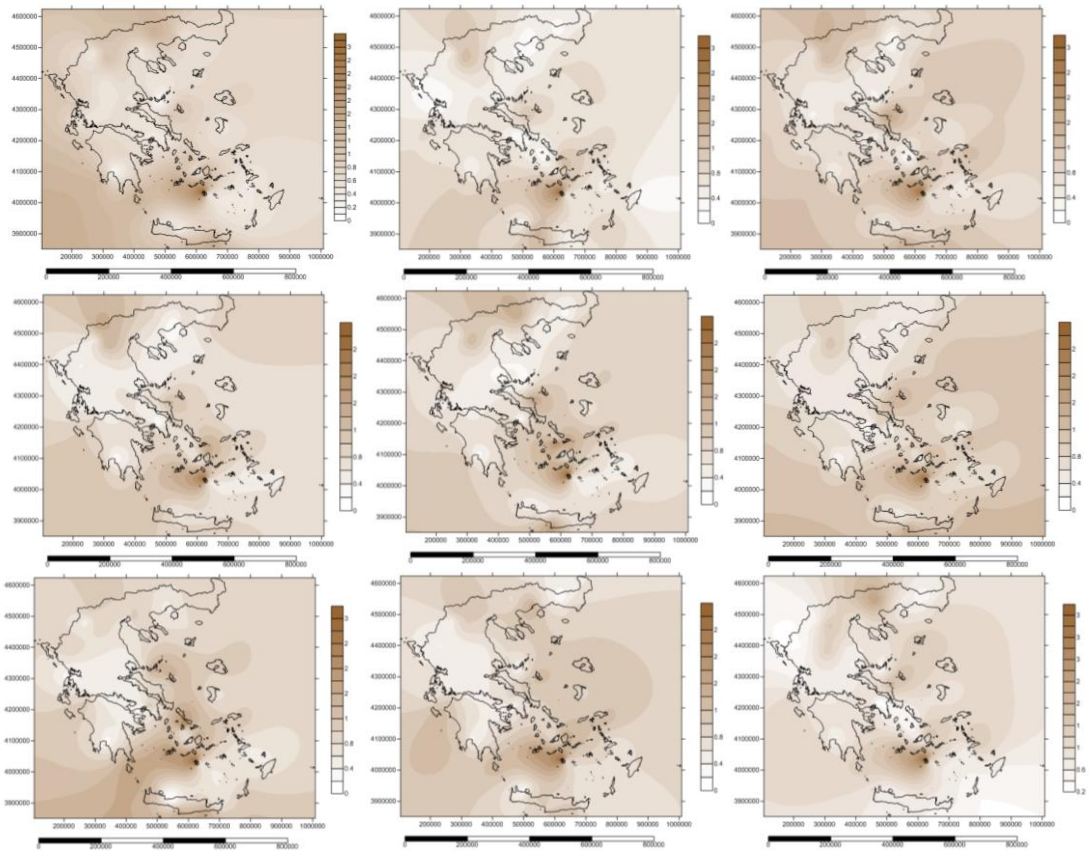

Figure 20: Disperse of the Weibull scale parameter (c, (m/s)), from monthly aggregated time series, at Greece, from January (top left) to December (bottom right, following right direction when reading).

Weibull parameter estimation (k, c)

Parameters of Weibull distribution shape (k) and scale (c (m/s)) ones were estimated through four different approaches, in order to deal with the best fit to the empirical sample. The selected stations were the same as the ones were used for the model fitting and the parameters estimated methods which were used were: (a) M.L.E. (Maximum Likelihood Estimator) (b) L – moments (c) Logarithmic transformed moments (L.T.M.) and (d) Graphical estimation. Results from the above mentioned methods were depicted to a diagram (fig. 21-23), as well as the empirical distribution of the data, from a specific station (Alexandroupoli). The diagram discloses which method best fits to the empirical data, by the shape of Weibull distribution, with parameters estimated from different approaches. The diagram manifested that all the above mentioned estimated methods gave very good approaches. As it is depicted at (Fig. 24-26), MLE and L-moments estimators were not affected by extreme values, so they appeared to be more accurate when estimating distribution's parameters.

Conclusionally, as MLE is a method based on optimization of the logarithmic likelihood function and also as L-moments are not affected by extremes, these two methods seemed to be the more accurate from the others. Finally, parameters estimated by MLE and L-moments methods were fitted better to the tail of empirical distribution, which is important especially for human structures and early warning measures due to extreme wind speed.

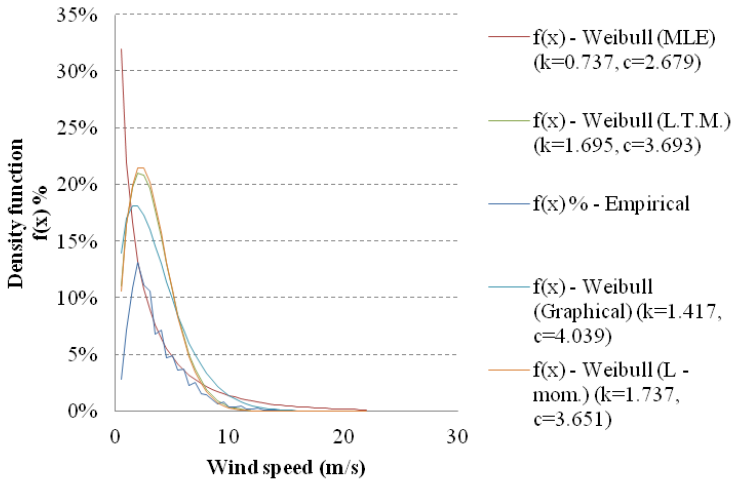

Figure 21: Estimation of Weibull parameters with for different approaches: (a) L – moments, (b) M.L.E. (c) Logarithmic Transformed Moments (L.T.M.) and (d) Graphical.

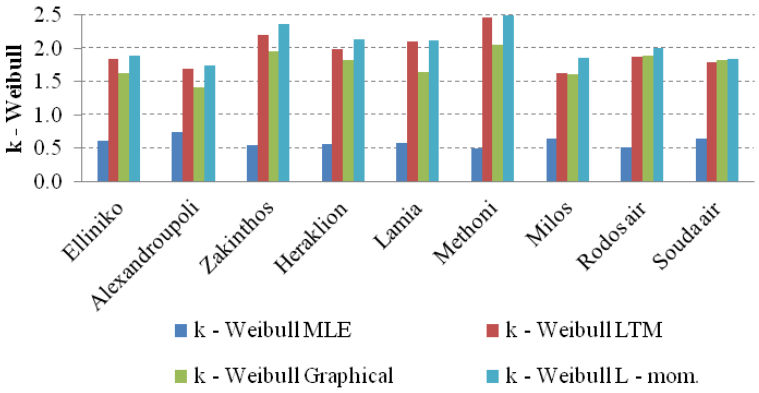

Figure 22: Comparison of Weibull shape (k), parameter estimation, from 9 stations and different estimated methods.

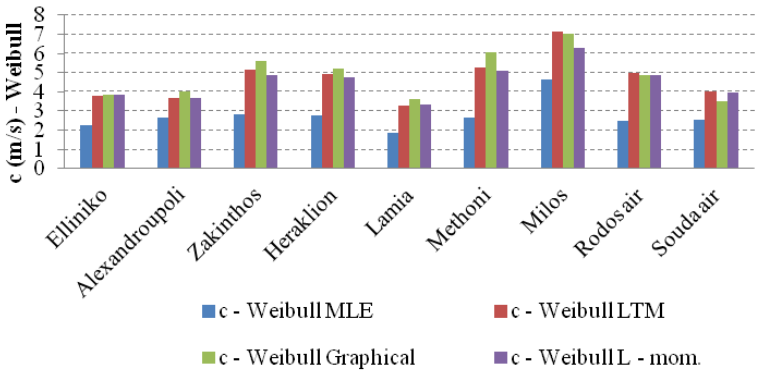

Figure 23: Comparison of Weibull scale (c (m/s)), parameter estimation, from 9 stations and different estimated methods.

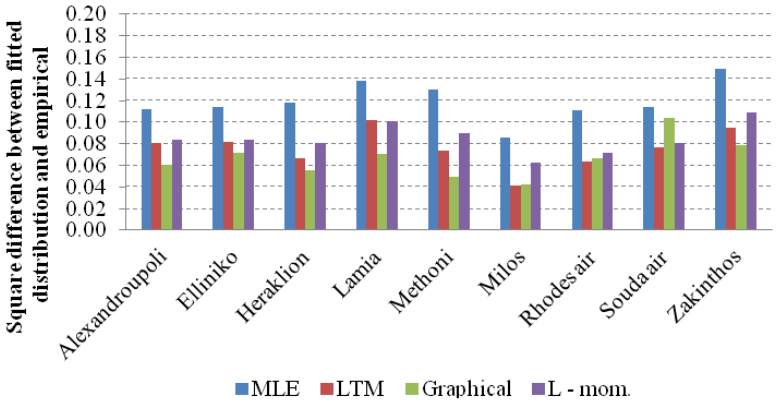

Figure 24: Square difference of fitted distribution and empirical one, of the 9 model estimated stations, with the four mentioned methods.

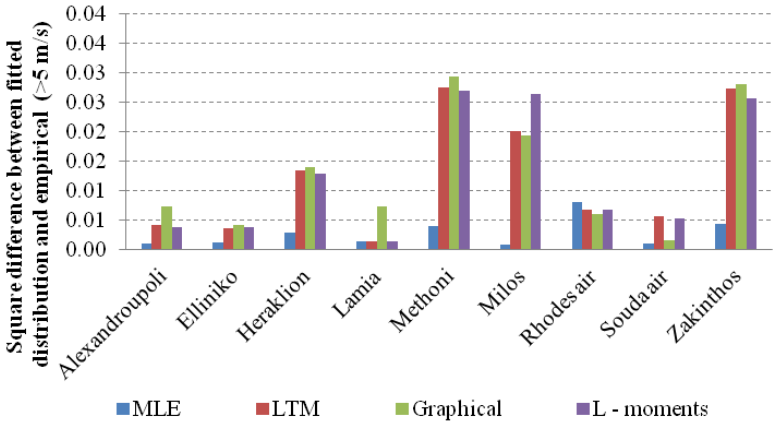

Figure 25: Square difference of fitted distribution and empirical one, of the 9 model estimated stations, with the four mentioned methods, for wind speed greater than 5 m/s.

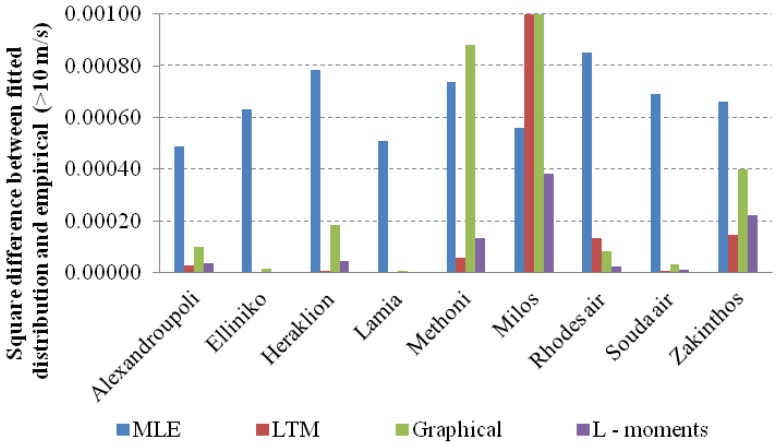

Figure 26: Square difference of fitted distribution and empirical one, of the 9 model estimated stations, with the four mentioned methods, for wind speed greater than 10 m/s.

From the 9 above estimated stations, it was concluded that the least square differences between fitted distribution (with the four mentioned methods) and empirical one, took the

minimum value for graphical method, for all data set. On the contrary, when the sample is clustered for wind speed over 5 and 10 m/s MLE and L-moments had the minimum square difference. Furthermore, due to the fact that in most cases we are interested in extreme wind speed events (energy, weather, early warnings), MLE (Fig. 25) and L-moments (Fig. 26) were found to be the best estimators for Weibull parameters.

Finding Hurst exponent for wind speed in Greece.

For all performed stations at daily time scale, climacograms were extracted (Fig. 27), from the standardized sample, in order to draw conclusions about the indirect finding of the persistence parameter of the wind speed and the direct calculation of the Hurst coefficient. It was found that climacograms of the examined stations have a relatively same slope, even at large time scale, which led to came up with a specific value of the Hurst coefficient for the entire region of Greece, $H = 0.75$.

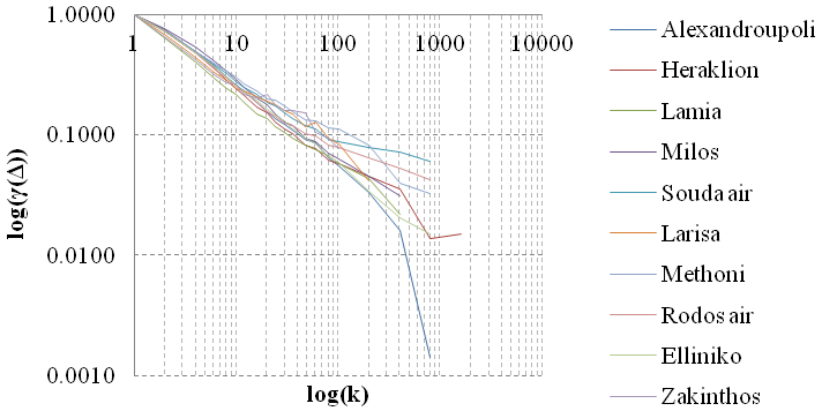

Figure 27: Climacogram, for 10 stations which were took place at wind speed modeling, at the standardized sample.

The above conclusion, led to the selection of 10 specific stations of the entire country, at daily time scale, based on the observed period, missing values and spatial variance of stations at the region of interest, thus conclusions, drawn from the exported model, to be generalized for the entire country. Specific maps were designed, in order to reveal the dispersion of the estimated model parameters (Fig. 28).

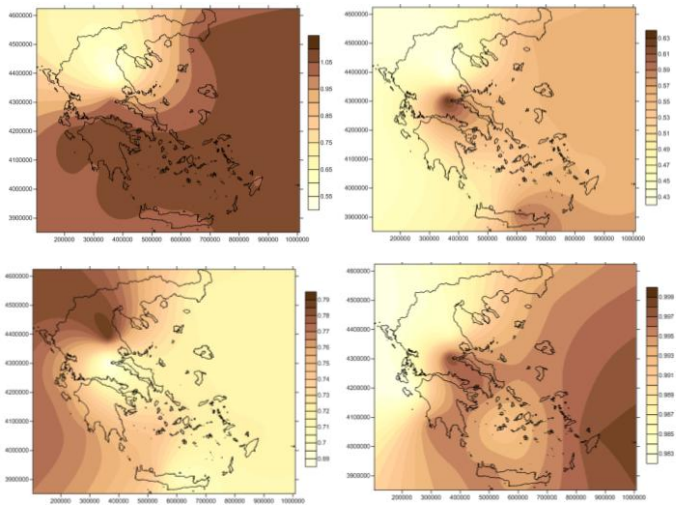

Figure 28: Dispersion of the (a) a = γ_0 parameter, (b) b = 2H-2, parameter, (c) Hurst exponent and (d) model fitting.

The estimation of the standard deviation (variance), was calculated by the unbiased estimator of the variance (Eq. 1, 2) and was adjusted to the selected 10 stations of the standardized data sample (Fig. 29, 30), which, as demonstrated in thesis (Koutsoyiannis, 2003), proved to be the most reliable estimator, contrary to autocorrelation function and spectra (pseudo-spectrum).

$$\mathrm{E}\left[\underline{\hat{\gamma}}(\Delta)\right] = \eta(\Delta, T)\gamma(\Delta) \quad (1)$$

$$\eta(\Delta, T) = \frac{1-\gamma(T)/\gamma(\Delta)}{1-\Delta/T} = \frac{1-(\frac{\Delta}{T})^2\Gamma(T)/\Gamma(\Delta)}{1-\Delta/T} \quad (2)$$

Where,

$E\left[\underline{\hat{\gamma}}(\Delta)\right]$: unbiased estimator of the variance

$\eta(\Delta, T)$: unbiased coefficient

γ(Δ): theoretical variance of the sample to the correspondence time scale (Δ)

γ(T): theoretical variance of the sample to the correspondence time scale (T)

Δ: relevant scale calculation

T: entire scale calculation for all data sample

Γ(T): autocovariance function for the discrete time process at time scale (T)

Γ(Δ): autocovariance function for the discrete time process at time scale (Δ)

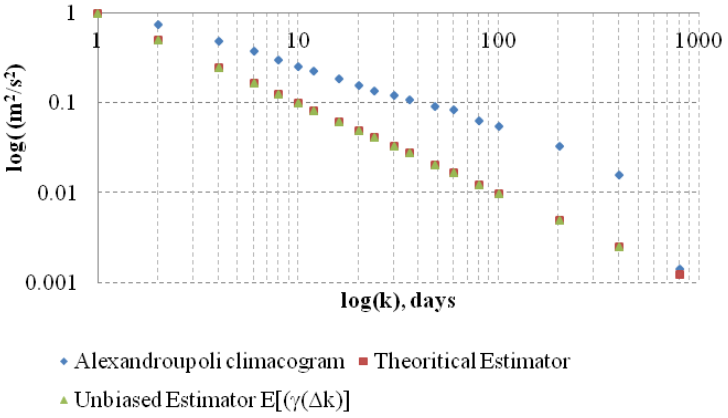

Figure 29: Climacogram of the theoretical, estimated and unbiased estimated variance (m/s) ^{2}, of Alexandroupoli station.

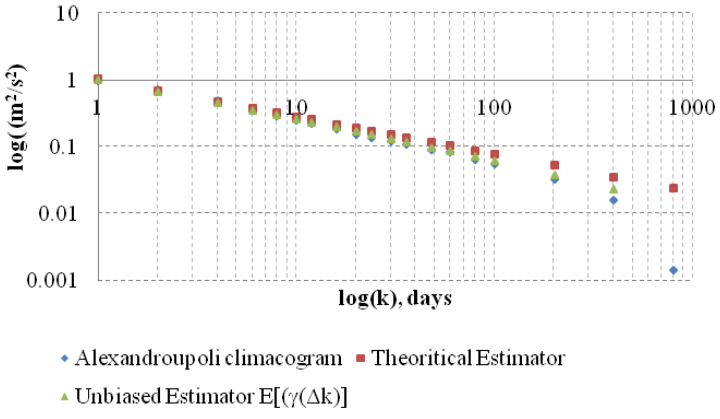

Figure 30: Fitted the unbiased estimator of variance$E\left[\underline{\hat{\gamma}}(\Delta)\right]$, to the empirical one γ (Δ), of Alexandroupoli station.

Furthermore, Hurst coefficient was estimated from climacograms directly from the empirical data from 10 stations and the results were compared to the unbiased estimated ones. The results seemed to be approximately equal (Fig. 31).

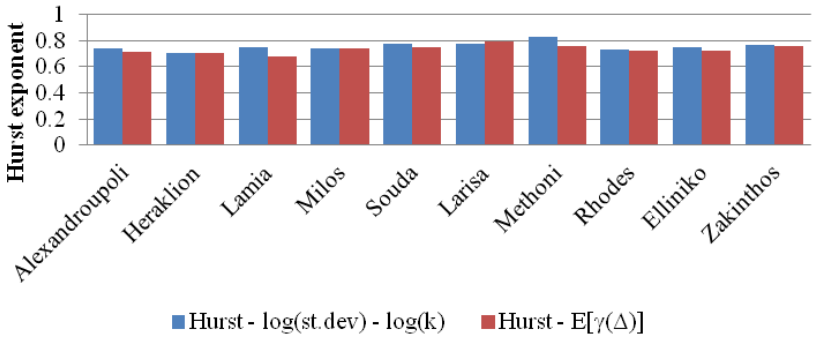

Figure 31: Compared Hurst exponent with empirical climacogram data standard deviation [log (st.dev.) – log (k)], (blue) and with unbiased variance estimator$E[\underline{\hat{\gamma}}(\Delta)]$, (red).

Synthetic time series generation

Synthetic time series, were generated from a particular station (Alexandroupoli), through the process of simple scaling model (Koutsoyiannis, 2002), which presented, the three ways, in which it became possible to produce a synthetic time series from Markov models, adapted to FGN ones, as well as maintain the desired statistical characteristics and persistence (Hurst coefficient) of selected time series. A description of the three methods was held and furthermore, was performed the process of random variations at multiple time scales, wherein, three AR (1) models were summed for the generation of a synthetic time series. Time series, which were extracted from these models, were fitted to normal distribution (production of AR (1) with adaptation to FGN), which does not correspond to the actual behavior of the wind (Fig. 30), which on a daily time scale, Weibull distribution is best adjusted. For that reason, suitable normal transformations were used, which adjusts any distribution to the normal one, tested with means of mean square error (RMSE), resulting from the adjustment of the inverse cumulative distribution function $(CDF)^{-1}$ on a diagram (Q - Q). The procedure mentioned above, was performed for finding the parameters of the used transformation Z (g(x)) and then, by performing the inverse transformation Z $(g(x))^{-1}$, the synthetic time series (which follows normal distribution) were denormalized and so a synthetic time series was generated (Fig. 32-36). Five transformations were applied and results of the generated - denormalized time series appeared at (Fig. 37-40).

Five normalized transformations were fitted to the empirical data in order to estimate their parameters through the gauge of least square error at Quantile-Quantile plot. After the parameter's estimation, the inverse process was held of de-normalized synthetic time series, in order to readjust to the distribution that empirical data follows. The five transformations which used were:

$$Z(t) = \left[aX(t)^{-\zeta} + \beta\right]\left(\gamma + \sqrt{\left(1+\frac{1}{\delta}\right) ln\{1+\delta[X(t)-\gamma]^2\}}\right) \quad (3)$$

(Papalexiou *et al.*, 2007), with five parameters (α, β, γ, δ, ζ)

$$\mathrm{Z} = \mathrm{g(x)} = \lambda\left[1+\left(\frac{x}{\nu}\right)^{-\theta}\right]\sqrt{\left(1+\frac{1}{\kappa}\right)} ln\left[1+\kappa\left(\frac{x}{\lambda}\right)^2\right] \quad (4)$$

(Koutsoyiannis et al., 2011), with four parameters (θ, κ, λ, ν)

$$Z = g(X) - g(0);\ g(x) = c + \mathrm{sgn}(x - c)\,\lambda\sqrt{\left(1+\frac{1}{\kappa}\right) ln\left[1+\kappa\left(\frac{x-c}{\lambda}\right)^2\right]} \quad (5)$$

(Koutsoyiannis et al., 2008), with three parameters (κ, λ, c) and when c=0:

$$Z = g(X) - g(0);\ g(x) = \mathrm{sgn}(x)\lambda\sqrt{\left(1+\frac{1}{\kappa}\right) ln\left[1+\kappa\left(\frac{x}{\lambda}\right)^2\right]} \quad (6)$$

$$y_i^{\lambda} = \begin{cases} y_i^{\lambda}; & \lambda \neq 0 \\ \log(y_i); & \lambda = 0 \end{cases} \quad (7)$$

(Box – Cox, 1964), with λ parameter

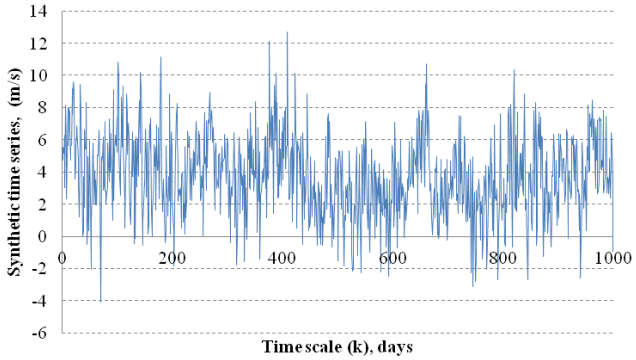

Figure 32: Generated synthetic normalized, time series, from Alexandroupoli station, from the multivariate time scale method. (Koutsoyiannis, 2002).

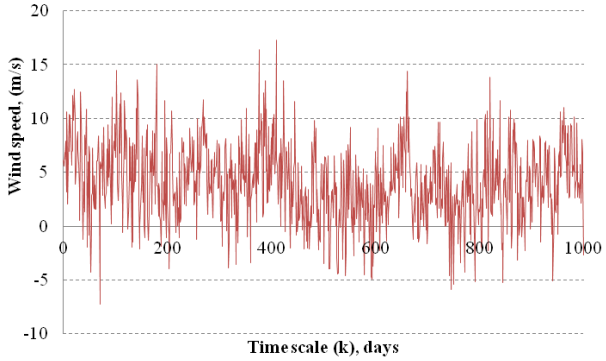

Figure 33: Generated synthetic de - normalized, time series, from Alexandroupoli station, from the normalized transformation proposed by (Papalexiou *et al.*, 2007).

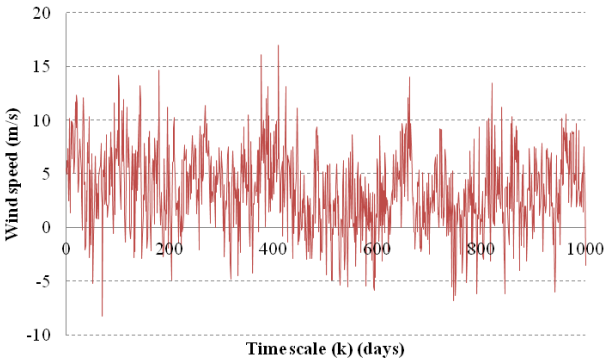

Figure 34: Generated synthetic de - normalized, time series, from Alexandroupoli station, from the normalized transformation proposed by (Koutsoyiannis et al., 2011).

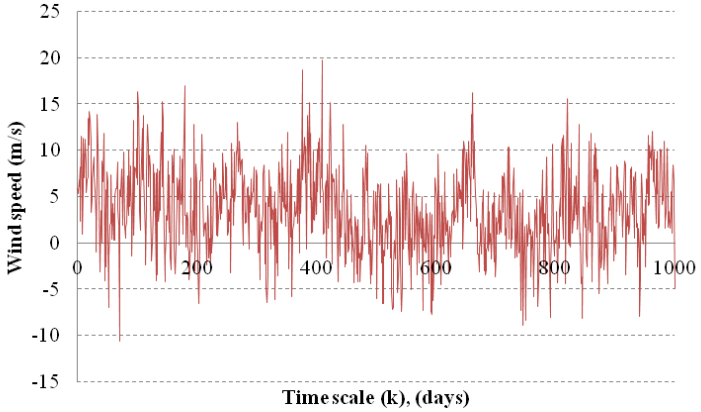

Figure 35: Generated synthetic de - normalized, time series, from Alexandroupoli station, from the normalized transformation proposed by (Koutsoyiannis et al., 2008).

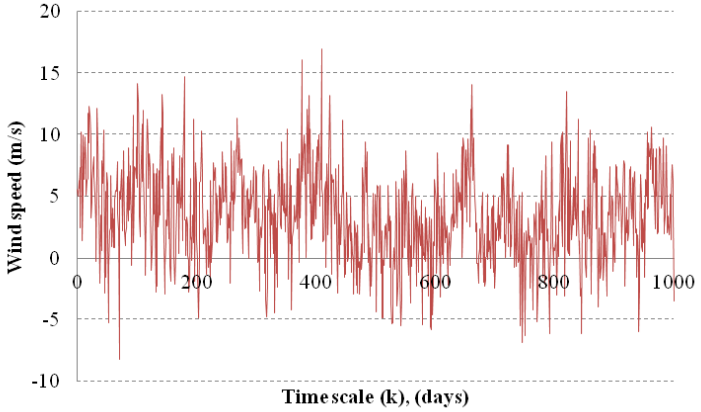

Figure 36: Generated synthetic de - normalized, time series, from Alexandroupoli station, from the normalized transformation proposed by (Koutsoyiannis et al., 2008).

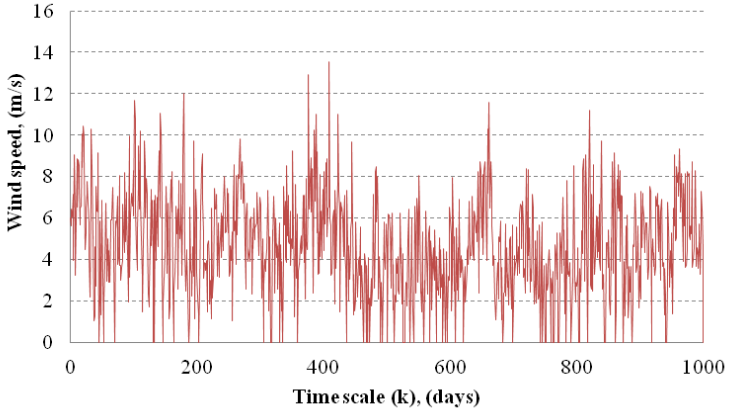

Figure 37: Generated synthetic de - normalized, time series, from Alexandroupoli station, from the normalized transformation proposed by (Box - Cox, 1964).

Specific transformations Z (g(x)) where used in order to normalize the empirical data of the selected station (Alexandroupoli), thus fitting data into Gauss distribution, which is a linear form at Quantile - Quantile plot. Quantile is an expression for the inverse cumulative

distribution and with minimizing the RMSE of empirical data with the $(CDF)^{-1}$ observed data were fitted to the normal inverse cumulative distribution. At the end of the above procedure, parameters of the transformations were estimated, which tend to be useful at the next inverse procedure, de - normalization of data, using the inverse transformation $Z\ (g(x))^{-1}$, which appeared at (Fig. 36-40).

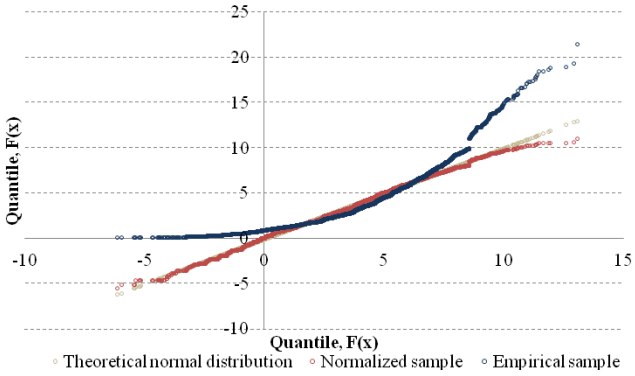

Figure 38: Empirical data (blue), which are fitted (red) to the inverse normal cumulative distribution (oil green) according to the transformation Z (g(x)) proposed by (Papalexiou *et al.*, 2007).

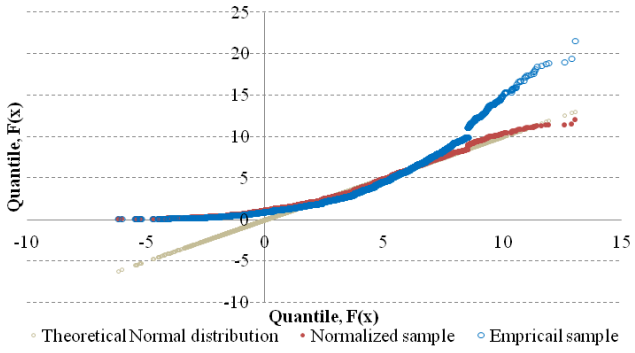

Figure 39: Empirical data (blue), which are fitted (red) to the inverse normal cumulative distribution (oil green) according to the transformation Z (g(x)) proposed by (Koutsoyiannis *et al.*, 2011).

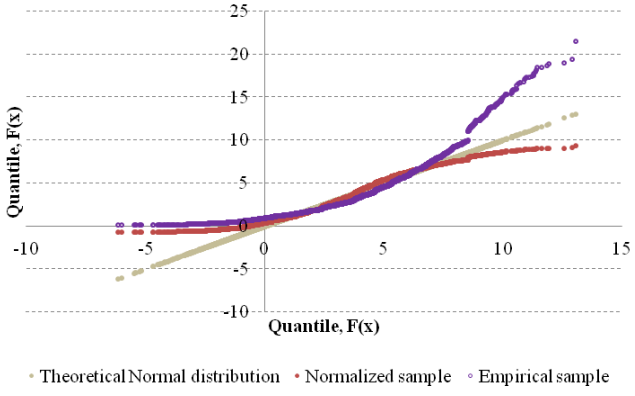

Figure 40: Empirical data (purple), which are fitted (red) to the inverse normal cumulative distribution (oil green) according to the transformation Z (g(x)) proposed by (Koutsoyiannis *et al.*, 2008).

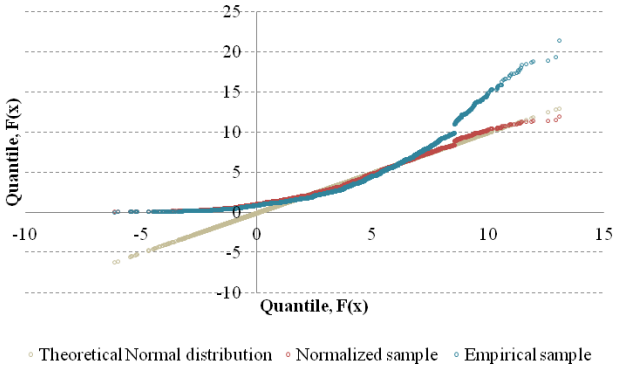

Figure 41: Empirical data (light blue), which are fitted (red) to the inverse normal cumulative distribution (oil green), according to the transformation Z (g(x)) proposed by (Koutsoyiannis *et al.*, 2008).

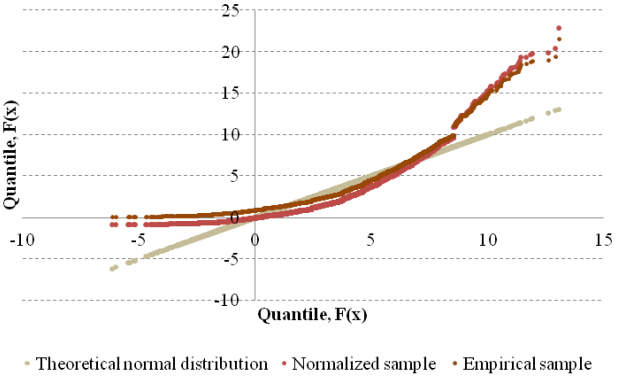

Figure 42: Empirical data (brown), which are fitted (red) to the inverse normal cumulative distribution (oil green), according to the transformation Z (g(x)) proposed by (Box – Cox, 1964).

In order to find which of the transformations, generates a synthetic time series which best fitted to the empirical data, by maintaining specific statistical characteristics as average, standard deviation and autocorrelation at lag = 1, a plot with the statistical characteristics for all of the five synthetic time series from each procedure mentioned above, was designed (Fig. 41), showing if empirical statistical characteristics from the observed data are maintained.

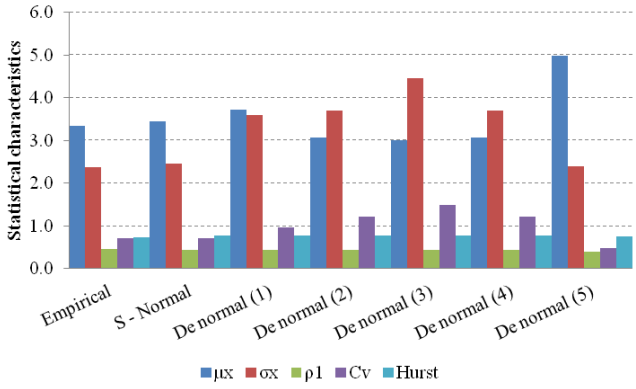

Figure 43: Statistical characteristics from empirical data, normal synthetic time series and five de – normalized synthetic ones, generated from different transformations.

Conclusions

From the statistical - stochastic analysis, some useful conclusions were extracted about the wind speed behavior in Greece.

- Southern and south - east areas of Greece are the windiest and especially the islands of the central Aegean (Naxos - Milos - Mikonos). Moreover, Rhodes Island and Methoni shows extreme wind episodes annually.
- Standard deviation seemed to keep pace with the same extreme areas mentioned above, as the differences of the maximum and minimum wind speed, makes these variable to be more dispersed.
- Southern and south - east areas seemed to have the higher theoretical wind energy, especially the islands of the central Aegean and also areas such as Methoni and Kithira seemed to have satisfactory wind energy.
- Reanalysis data seemed to be well cross correlated to the observed values, as well as, they imply the same regions of maxima and minima of the wind speed as the observed.
- Weibull distribution best fits the wind speed data, as well as GEV max distribution best fits to the gust.
- The estimation of Weibull's parameters, shape (k) and scale (c(m/s)) factor seemed to have a specific pattern, which reveals dependence to the area (islands – seashore – continental) and to seasonality (Winter – Autumn – Spring – Summer).
- The best estimator for Weibull's parameters seemed to be MLE and L-moments estimators, which are not affected by extreme values (outliers) of the observed data.
- Wind seemed to blow from northern direction at approximately 45% percentage while 60% of the mentioned percentage corresponds to February.
- Trends of wind speed showed from the period 1970-2013 that wind speed is reduced through years in central Greece with rate 0.05 m/s/month and increased to the rest of the area with rate 0.03m/s/month. Trends for periods 1970-1990 and 1991-2013 showed a reduction at rate 0.07 m/s/month and increment at rate 0.1 to 0.06 m/s/month respectively, for the same regions as the above mentioned.
- Catastrophic events seemed to follow, spatial and temporal wind speed trends. These extreme events appeared at almost the same regions with positive wind speed trends and also most of them are observed the last two or three decades.
- Hurst exponent was calculated from climacograms for all Greece and the value of H=0.75 seemed to fit observed data, well enough.

Appendices

Additionally, at the end of this assignment, there are three appendices in which are gathered the results of the above treatment. The appendix A (in Greek) pooled tables with data processing and the results of the calculations. The appendix B (in Greek), where maps are exported, for a better overview of the spatial distributed results, for monthly - annual and seasonal time scale and finally at the appendix C (in Greek), there are charts, bar charts, histograms and rose charts, to confirm the results and conclusions, drawn from this thesis.